

Laboratory Scale Seismic Surface Wave Testing for the Determination of Soil Elastic Profiles

A. Madun^{1,2*}, I. Jefferson², K.Y. Foo³, D.N. Chapman², M.G. Culshaw^{2,4} and P.R. Atkins³.

¹ Faculty of Civil and Environmental Engineering, University of Tun Hussein Onn, Malaysia.

² School of Civil Engineering, University of Birmingham, Edgbaston, Birmingham, B15 2TT, UK.

³ School of Electronic, Electrical and Computer Engineering, University of Birmingham, B15 2TT, UK.

⁴ British Geological Survey, Keyworth, Nottingham, NG12 5GG, UK.

Abstract: Seismic surface wave testing is well-adapted to the study of elastic parameters and, hence, the elastic profile of soils in the field. Knowledge of a ground's stiffness profile enables the prediction of ground movement and, thus, the quality of the foundation. The stiffness parameter obtained in this research corresponds to the measurement of the seismic surface wave phase velocity of materials, which relates to the very small strain shear modulus. This paper describes a methodology for performing surface wave testing in the laboratory. In comparison with field tests, a laboratory-scale experiment offers the advantage of allowing the process of data collection to be calibrated, and analytical studies can be carried out as the properties of the material under test are controllable and known *a priori*. In addition, a laboratory scale experiment offers insight into the interaction between the seismic surface wave, the soil, the boundary and, hence, the constraints associated with the seismic surface wave technique. Two simplified models of different sizes were developed using homogeneous remoulded Oxford Clay at different water contents and corresponding undrained shear strengths. The laboratory experimental methodology demonstrated that the seismic surface wave equipment used in the laboratory was directly influenced by the clay properties as well as the size of the test model. The methodology also showed that the arrangement of the seismic source and the receivers had an impact on the range of reliable frequencies and wavelengths obtained.

Keywords: Seismic surface wave testing, soil elastic profile, very small strain shear modulus

1. Introduction

Traditionally, the measurement of the stiffness profile of a soil is carried out by using laboratory and *in-situ*, invasive, field tests. However, the process of sample retrieval required for laboratory testing often introduces additional difficulties associated with sample disturbance and the reliability of the sample in representing the entire site. As a result, sample retrieval from the field for laboratory testing may not be sufficient in replacing field-testing. Penetration testing, dynamic probing and field vane shear tests are examples of conventional field-test techniques used to determine soil stiffness profiles. Geophysical methods, such as seismic surface wave techniques, offer a non-intrusive and non-destructive approach to carry out the very small strain stiffness profile measurements. Moreover, the seismic surface wave approaches provide a cost effective way to assess site conditions. A comparison between geophysical seismic-based techniques and conventional geotechnical load-testing methods for the measurement of the ground stiffness profile was presented by Matthews *et al.* [1], drawing the conclusion that geophysical testing can deliver results of significant quality. A stiffness parameter obtained from a seismic wave test is the maximum value occurring at very small strain (0.001 %).

At such strain levels most soils behave elastically and stiffness is independent of strain [2].

Civil structures need to be designed with adequate factors of safety, especially for a critical construction site, such as an excavation adjacent to other structures. Therefore, a realistic prediction of ground movement that may affect a structure is crucial. The use of small strain stiffness provides a way of doing this. Nowadays, a numerical modelling technique is commonly used to predict soil deformation, which uses a wide range of constitutive soil models. The seismic wave technique can provide a reliable estimate of stiffness since understanding of the relationship between the stiffness obtained from the seismic and conventional methods has been greatly improved [3]. Traditionally, the seismic wave technique has been used to ascertain soil profile as well as for anomalies detection, such as locating subsurface voids [4]. In addition it can be used in quality testing in ground improvement works [5]. Thus it is essential that a fuller understand of surface wave analysis and interpretation take place.

The understanding of the seismic surface wave profiles in relation to soil properties at the laboratory scale is highlighted in this paper. The aim of this paper is to describe a development of the methodology for

*Corresponding author: : aziman@uthm.edu.my

performing surface wave testing in the laboratory. In comparison with field tests, a laboratory-scale experiment offers the advantage of allowing the process of data collection to be calibrated and analytical studies can be carried out as the properties of the material under test are controllable and known *a priori*. The experimental set-up is described, followed by the data processing, seismic results and calibration with physical tests before drawing the appropriate conclusions.

2. Theoretical Background

When the ground surface is vibrated with a vertical load, two-thirds of the energy is transformed into surface waves and propagated parallel to the ground surface. Rayleigh waves form as a result of interfering P and S waves at the ground surface [6]. Surface waves have dispersive characteristics and thus, can be utilised to identify near-surface elastic properties. Dispersion arises because different frequencies or wavelengths travel at different depths. In homogeneous material, surface wave velocity does not vary with frequency. However, in layered soils with different densities, surface wave velocity varies with frequency where there is a variation in stiffness with depth [7]. This phenomenon explained by the layering medium illustrated in Figure 1, where medium 1 with thickness L overlying medium 2. The Rayleigh wavelength (λ_1) shorter than L would propagate mainly within the medium 1, thus phase velocity is representative medium 1. However, the Rayleigh wavelength (λ_2) is larger than L and this occurs as the phase velocity is influenced by the properties of both medium 1 and 2 [8]. This phenomenon is called dispersion, causing different frequencies and wavelengths to travel at different velocities.

The surface wave method generally can be separated into two main steps of data collection and signal processing for spectral analysis. For data collection, there is usually a seismic source, generating a signal $x(t)$, and multiple receivers deployed to acquire the seismic data, represented by $y_1(t) \dots y_n(t)$ where n is the index of the array of receivers. The common options for a seismic source are usually a manually controlled mass dropped to induce a broadband impulsive signal into the ground, or an electro-mechanical shaker controlled by a digital source. The earlier option is the simplest, while the latter allows precise control and variations of the source signal characteristics both in terms of bandwidth and time duration. The receivers usually consist of geophones for field testing, or accelerometers in laboratory-scale testing.

For signal processing and spectral analysis, the time-domain signals are discretely sampled, $y_n(k)$, by an analogue-to-digital converter and N -points are stored on a computer where the processing and the subsequent spectral analysis are carried out. To adequately capture the spectrum of the signals, the sampling rate, f_s , of the analogue-to-digital converter should be at least twice the maximum bandwidth of the signal, and usually higher in

practice. The Discrete Fourier Transform (implemented using the FFT [Fast Fourier Transform] algorithm) is then applied to the signal to obtain the discrete spectrum of the signal, $Y_n(f)$:

$$Y_n(f) = \sum_{k=0}^{N-1} y_n(k) \exp(-j2\pi f k/N) \quad (1)$$

where f is the discrete frequency of the signal, $N = Tf_s$, while k and T are the discrete-time and time-duration of the signals. The signals are usually zero-padded in the time-domain prior to the application of a radix-2 FFT algorithm. The phase velocity, as a function of frequency, between any two receivers, can be calculated from their corresponding phase difference. The phase difference at a particular frequency, $\Delta\phi(f)$, is the angle of the complex spectrum value, and expressed as:

$$\Delta\phi_{mn}(f) = \tan^{-1} \left(\frac{\text{Im}(S_{mn}(f))}{\text{Re}(S_{mn}(f))} \right) \quad (2)$$

where m and n are the paired receivers for which the phase difference is calculated. It should be noted that using only a single phase difference measurement is usually more prone to error from noise and interference from other modes of wave propagation. Therefore, it is recommended that if the signal-to-noise ratio is sufficiently high across reasonable bandwidths, then a best fit phase-frequency gradient is used as a method of averaging to calculate the time-delay.

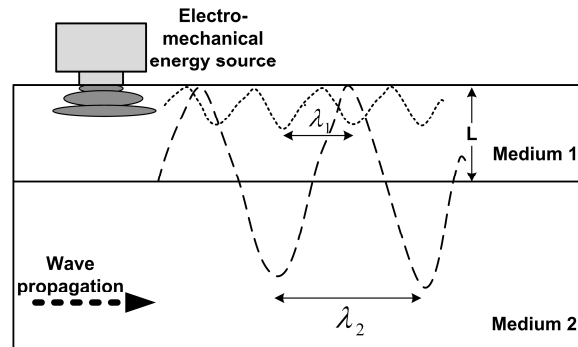


Figure 1: Rayleigh waves dispersion [8].

The time-delay associated with the phase difference observed between the two receivers can be derived from [9]:

$$\tau(f) = \frac{\Delta\phi(f)}{2\pi f} \quad (3)$$

The frequency-dependent phase velocity, $v(f)$, can then be obtained using the distance between the two receivers m and n , $\Delta_{mn}x$, such that [9]:

$$v_{mn}(f) = \frac{2\pi f \Delta_{mn}x}{\Delta\phi_{mn}(f)} \quad (4)$$

The plot of phase velocity versus frequency is the dispersion curve. To obtain the phase velocity with respect to wavelength is using direct relationship of [9]:

$$\lambda(f) = \frac{v(f)}{f} \quad (5)$$

Where $\lambda(f)$ is a wavelength. In a solid and homogeneous medium, the Rayleigh-wave phase velocity, v_r , can be converted into shear-wave velocity, v_s , which for an elastic medium is approximately:

$$v_s \cong \frac{1 + \nu}{0.862 + 1.14\nu} v_r \quad (6)$$

where ν is a Poisson's ratio [10]. The maximum shear modulus of the material, G_{max} , which describes the behaviour of the ground under load [11], is related to the mass soil bulk density, ρ , and the shear wave velocity through the relationship:

$$G_{max} = \rho v_s^2 \quad (7)$$

Using the above relationships, the measurements of the Rayleigh-wave phase velocity enables the evaluation of the stiffness profile of the ground, as well as the associated effect of the improvement work that had been carried out.

The wavelength penetration depth is based upon the assumption that the amplitude of the surface wave is attenuated linearly as a function of depth, and can usually be represented by a direct relationship of:

$$D \approx k\lambda(f) \quad (8)$$

where the wavelength, $\lambda(f)$, is

$$\lambda(f) = \frac{v(f)}{f} \quad (9)$$

The k represent constant dependent upon the tested material homogeneity and could be 0.25, 0.33, 0.5 and 1 as reviewed by Addo and Robertson [12] and Matthews *et al.* [2]. The k value 1 is commonly used for a vertically homogeneous site and has been used in this study.

3. Experimental Set-Up and Calibration

The purpose of performing a laboratory-scale experiment, instead of a field test, is that the process of data collection can be pre-calibrated, and that the true data regarding the material can be measured *a priori*. In this setup, two sizes of containers were constructed measuring (1): 600 mm x 300 mm x 300 mm and (2): 1080 mm x 680 mm x 500 mm in length, width and depth respectively. The containers contained Oxford Clay (using samples taken from a site near Peterborough, in the Midlands region of the UK) at different water contents of 32 % and 40 %. At both water contents, samples were tested using Quick undrained triaxial test and gave shear strength of 33 kPa and 16 kPa respectively. The Oxford Clay was compacted in layers using a vibrating hammer. A plastic sheet was used to cover the top of the container to minimize water evaporation.

The array of receivers consisted of up to 4 piezoelectric accelerometers. The seismic source was located at the middle of the sensor-pairs. The distance between the

source and the first receiver, d , was set as 5 cm and receiver spacing, Δx , was 2.5 cm for the smaller container. Meanwhile, d was set as 7 cm and Δx was 3 cm for the larger container. The stepped-frequencies applied ranged from 100 Hz to 10 kHz for the smaller container and 50 Hz to 3000 Hz for the larger container.

An illustration of the laboratory set-up is shown in Figure 2. A script was written within the Matlab environment to conduct the experiment using a computer. The computer was connected to a National Instruments data acquisition system, in which a 16-bit analogue output module (NI-9263) generated the transmission waveforms. An audio power amplifier was used to drive the vibrator with the excitation signals. On the receiving side, the sensors consist of four piezoelectric accelerometers (ICP 352C42 by PCB Piezotronics) with a frequency range of 1 Hz to 10 kHz that were coupled to the surface with 1 cm length nails. The accelerometers were connected to an analogue signal conditioner and were then sampled by a 24-bit sigma-delta analogue-to-digital converter module (NI-9239) with a sampling rate of 50 kHz. Collected data were stored, and processed after the completion of a data acquisition session. To minimise ambient noise, the container was isolated from the ground with acoustic absorbers.

4. Data Processing and Result Analysis

After the completion of each data collection session, the data were loaded into Matlab for processing. The first step was to apply a Fast Fourier Transform (FFT) on all the data to obtain the spectral representation of the received signal. The results were a series of complex values of which the magnitude and angle, respectively, represent the spectral amplitude and phase. As a stepped-frequency transmission was implemented, the complex value corresponding to the frequency of transmission with which the received signal is associated was selected and stored. This was repeated for all transmissions at the same frequency, and then for all the frequency steps across the whole range. This yielded a new spectral series of complex FFT values as a function of the stepped frequencies. Therefore, the data were reduced to the stepped-frequency spectral representation for the 4 sensor channels, with 5 multiple sets as there were 5 repetitive snapshots for each frequency step during data acquisition. The next step was to obtain the phase difference between the receivers. Among the 4 sensors, there were 2 phase difference measurements between sensor pairs; A-B and C-D. For each of these adjacent sensor pairs, the phase difference was obtained by performing a complex conjugate multiplication in the spectral domain. For example, to obtain the phase difference between adjacent sensors A and B, the FFT of signal from sensor A was multiplied by the complex conjugate of the FFT of signal from sensor B. Since there were multiple snapshots, the spectra used in the multiplications were that of the average.

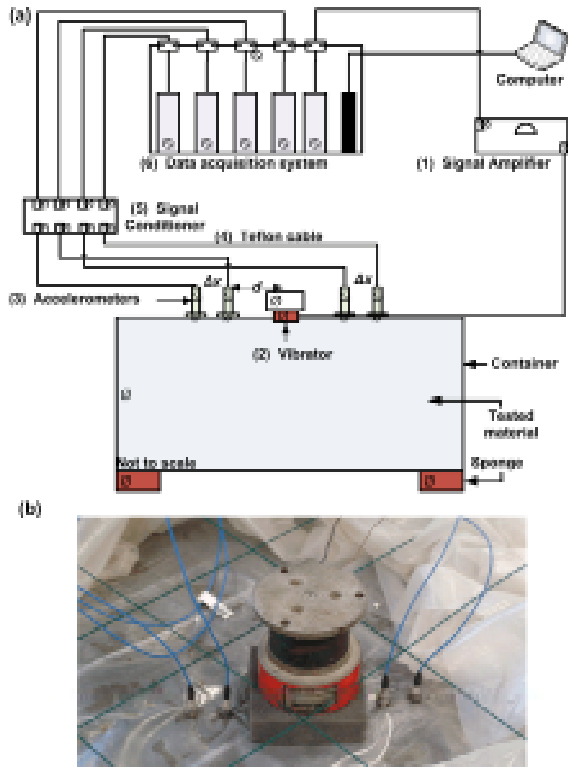


Figure 2: (a) Illustration of the laboratory-scale model and equipment set-up, and (b) photo of the Oxford Clay with sensing accelerometers where the seismic source was located at the centre of the array.

In general, both unwrapped phase differences shown in Figure 3(a) and (b) were a linear function. The reliable frequencies for unwrapped phase difference for smaller and larger containers were laid from 633 to 3796 Hz and 216 to 1297 Hz respectively. Therefore for Figure 2(a) and 2(b), the reliable phase difference should be on that ranged of frequencies. Data outside that ranged were considered unreliable due to the effect of noise and of body wave.

For example the linear plot 3(a) shows a larger deviation beyond the frequency of 6000 Hz due to a reduction of signal quality, as these frequencies correspond to wavelengths that exceed the distance constraints of the sensors with respect to the source.

The phase velocities were averaged between both pair of transducers. The plots of phase dispersions show a similar trend of consistency, as illustrated in Figures 4 and 5 respectively. The deviation in phase velocities was not caused by a change of soil properties, but caused by the frequencies/wavelengths constraint that influences the near and far-offset distance of the source from the receivers, as well as some reflected waves from the boundary of the soil container. The phase velocities in Figure 4 are relatively consistent at frequencies between 600 and 6000 Hz. Above 7000 Hz the phase velocities were corrupted due to a reduction of signal quality. Meanwhile in Figure 5, phase velocities are relatively

consistent across the frequencies. Unusual phase velocities occurred for frequencies below 600 Hz and 200 Hz in Figures 4 and 5 respectively, which are likely affected by the body wave.

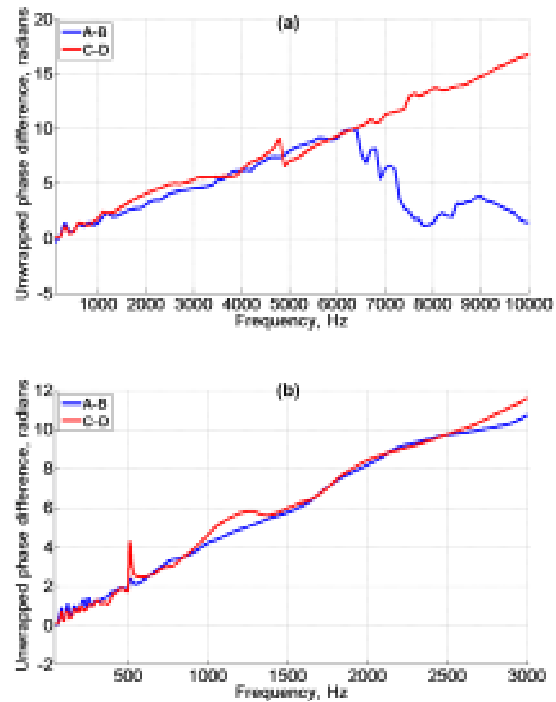


Figure 3: Graph of unwrapped phase difference for (a) smaller container filled with clay at 32 % water content and (b) larger container at 40 % water content.

The shear strength (c_u) was used to estimate shear wave velocity (V_s) via empirical conversion, $c_u = 0.0424v_s^{1.462}$, as established by Mattsson *et al.* [13]. The shear wave velocities were then converted to phase velocities (v_r) using Equation 6, $v_r = 0.955 \cdot v_s$, with the assumption that the Poisson's ratio for clay is 0.5. The shear strength of Oxford Clay at 32 % and 40 % water content were 33 kPa and 16 kPa and, using the above conversion, the calculated phase velocities were 91 m/s and 55 m/s respectively. These converted phase velocities were close to the average measured phase velocities.

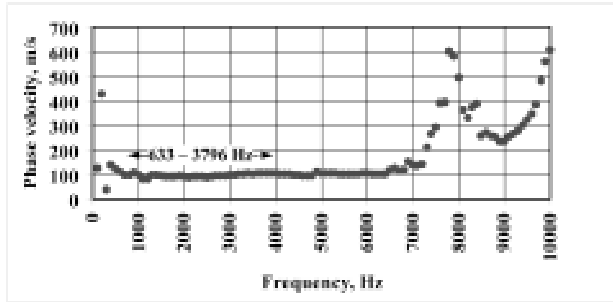


Figure 4: Graph showing variation of phase velocities across the frequencies from the test conducted on the smaller container filled with clay at 32 % water content.

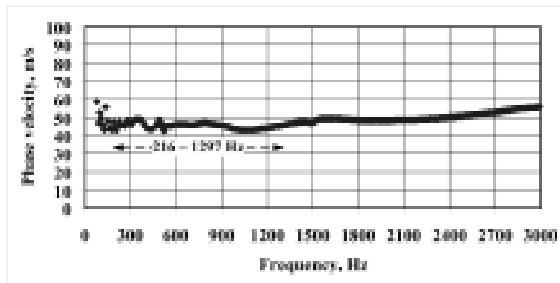


Figure 5: Graph showing variation of phase velocities across the frequencies from the test conducted on the larger container filled with clay at 40 % water content.

The measured phase velocities were converted to shear wave velocities using equation 6. The maximum shear modulus, G_{max} , was calculated using equation 7. It is worth noting that the clay with water contents of 32 % and 40 % had bulk densities of 1820 kg/m^3 and 1711 kg/m^3 respectively. The maximum shear modulus plots versus wavelength for homogeneous Oxford Clay at 32 % and 40 % water content, are shown in Figure 6 and 7 respectively. The measurements demonstrate that the clay in the two containers had very different shear moduli, which indicated that the surface wave technique was reliable to carry out at the laboratory scale using the equipment and methodology described in this paper. This outcome is important for future utilisation of the equipment and methodology in understanding the surface wave results when conducting further tests on different ground models.

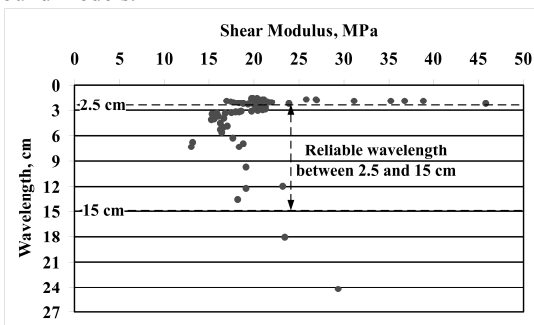


Figure 6: Shear modulus versus wavelength for measurements conducted on the smaller container filled with Oxford Clay at 32 % water content.

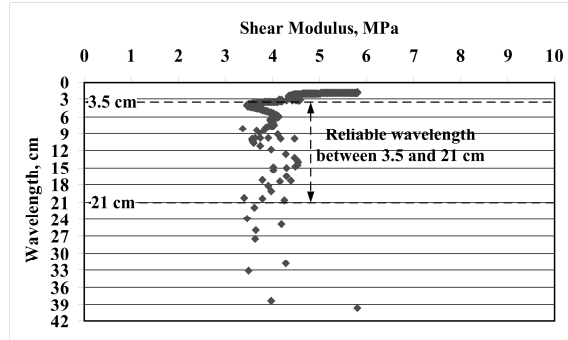


Figure 7: Shear modulus versus wavelength for measurements conducted on the larger container filled with Oxford Clay at 40 % water content.

5. Discussion

The arrangement of the transmitter and receiver arrays is subject to the near and far offset constraints [14]. The larger range of frequency offered the advantage of being able to select the useful wavelengths that fulfill the frequency/wavelength constraint. These constraints are associated with the wavelength of the signals and, therefore, determine the maximum and minimum frequencies/wavelengths that are useful for spectral analysis. The near-offset constraint empirical rule for the maximum wavelength (λ_{max}) is recommended in the literature [1], [15], [16], [17] as a function of the distance from the source to the first receiver, d , to be approximately:

$$\lambda_{max} < 3d$$

The far-offset is associated with the attenuation of the surface waves when the receiver is far away from the seismic source. This constraint is approximately:

$$\lambda_{min} > d/2$$

λ_{min} and λ_{max} are the wavelengths corresponding to the minimum and maximum frequencies respectively. Therefore, the reliable shear modulus plot in Figures 6 and 7 were constrained between these wavelengths. For the smaller container the reliable wavelengths were between 2.5 and 15 cm, and for the larger container between 3.5 and 21 cm. Meanwhile, the reliable frequencies calculated using average phase velocities for Oxford Clay in equation 5 were between frequencies of 633 and 3796 Hz for the smaller container and between 216 and 1297 Hz for the larger container, as shown in Figures 4 and 5. The reliable ranges of frequencies/wavelengths observed, showed consistency in the phase velocities, which indicate that the Oxford Clay in both containers was in a homogeneous condition.

6. Conclusion

The feasibility of using surface wave testing equipment and its analytical system at laboratory scale has been demonstrated. A laboratory experiment scaled from a typical soft clay site was carried out using remoulded

Oxford Clay with known physical properties and therefore allowing detailed evaluation and comparison. The average phase velocity and shear modulus measured for remoulded Oxford Clay at 32 % moisture content were 94.9 m/s and 18.1 MPa respectively. Meanwhile remoulded Oxford Clay at 40 % moisture content were 45.4 m/s and 3.9 MPa respectively. These phase velocities were in agreement with the converted phase velocities using undrained shear strengths of 91 m/s and 55 m/s respectively.

ACKNOWLEDGEMENT

The authors would like to thank the University of Tun Hussein Onn, Malaysia, and the Ministry of Higher Education, Malaysia, for their generous sponsorship of this research.

REFERENCES

- [1] Matthews, M.C., Hope, Y.S. and Clayton, C.R.I. (1995). "The geotechnical value of ground stiffness determined using seismic methods." *Geological Society, London, Engineering Geology* Special Publication, 12, pp. 113-123.
- [2] Matthews, M.C., Hope, Y.S. and Clayton, C.R.I. (1996). "The use of surface waves in the determination of ground stiffness profiles." *Proceedings of the Institution of Civil Engineers Geotechnical Engineering*, 119, pp. 84-95.
- [3] Clayton, C.R.I. (2011). "Stiffness at small strain: research and practice." *Géotechnique*, 61 (1), pp. 5-37.
- [4] Xu, C. and Butt, S.D. (2006). "Evaluation of MASW techniques to image steeply dipping cavities in laterally inhomogeneous terrain." *Journal of Applied Geophysics*, 59, pp. 106– 116.
- [5] Moxhay, A.L., Tinsley, R.D. and Sutton, J.A. (2001). "Monitoring of soil stiffness during ground improvement using seismic surface waves." *Ground Engineering Magazine*, pp. 34-37.
- [6] Xia, J., Miller, R.D., Park, C.B., Hunter, J.A., Harris, J.B. and Ivanov, J. (2002). "Comparing shear wave velocity profiles inverted from multichannel surface wave with borehole measurements." *Soil Dynamics and Earthquake Engineering*, 22, pp. 181-190.
- [7] Stokoe, K.H., Wright, G.W., Bay, J.A. and Roesset, J.M. (1994). "Characterisation of geotechnical sites by SASW method." *In: Woods, R.D. (ed) Geophysical Characterisation of Sites*. New York: Oxford Publishers.
- [8] Rhazi, J., Hassaim, M., Ballivy, G. and Al-Hunaidi, M.O. (2002). "Effects of concrete non-homogeneity on Rayleigh waves dispersion." *Magazine of Concrete Research*, 54(3), pp. 193–201.
- [9] Phillip, C, Cascante, G and Hutchinson, D.J. (2004). "Shear-wave velocity measurement of soils using Rayleigh waves." *Canadian Geotechnical Journal*, 29(4), 1992, pp. 558-568.
- [10] Richart, F.E., Wood, R.D. and Hall, J.R. (1970). "Vibration of soils and foundations." New Jersey: Prentice-Hall.
- [11] Matthews, M.C., Clayton, C.R.I. and Own, Y. (2000). "The use of field geophysical techniques to determine geotechnical stiffness parameters." *Proceedings of the Institution of Civil Engineers Geotechnical Engineering*, 143, pp. 31-42.
- [12] Addo, K.O. and Robertson, P.K. (1992). "Shear-wave velocity measurement of soils using Rayleigh waves." *Canadian Geotechnical Journal*, 29(4), pp. 558-568.
- [13] Mattsson, H., Larsson, R., Holm, G., Dannewitz, N. and Eriksson, H. (2005). "Down-hole technique improves quality control on dry mix columns." *In: Proceedings of the International Conference on Deep Mixing Best Practice and Recent Advances*, Stockholm, Sweden, Vol. 1, pp. 581-592.
- [14] Heisey, J.S., Stokoe, K.H. and Meyer, A.H. (1982). "Moduli of pavement systems from spectral analysis of surface waves." *In: Strength and deformation characteristics of pavements. Transportation Research Record 852, Transportation Research Board, National Research Council*, Washington, D.C., pp. 22–31.
- [15] Al-Hunaidi, M.O. (1993). "Insight on the SASW non-destructive testing method." *Canadian Geotechnical Journal*, 20, pp. 940–950.
- [16] Park, C.B., Miller R.D. and Xia, J. (1999). "Multichannel analysis of surface waves." *Geophysics*, 64(3), pp. 800-808.
- [17] Madun, A., Jefferson, I., Chapman, D.N., Culshaw, M.G., Foo K.Y. and Atkins, P.R. (2010). "Evaluation of the multi-channel surface wave analysis approach for the monitoring of multiple soil-stiffening columns." *Near Surface Geophysics*, 8(6), pp. 611-621.